Biochimica et Biophysica Acta 1858 (2016) 1110–1117

Contents lists available at ScienceDirect

Biochimica et Biophysica Acta

journal homepage: www.elsevier.com/locate/bbamem

Functional roles of MICU1 and MICU2 in mitochondrial Ca^{2+} uptake

Jessica Matesanz-Isabel, Jessica Arias-del-Val, Pilar Alvarez-Illera, Rosalba I. Fonteriz, Mayte Montero, Javier Alvarez *

Instituto de Biología y Genética Molecular (IBGM), Departamento de Bioquímica y Biología Molecular y Fisiología, Facultad de Medicina, Universidad de Valladolid and Consejo Superior de Investigaciones Científicas (CSIC), Ramón y Cajal, 7, E-47005 Valladolid, Spain

ARTICLE INFO

Article history:
Received 7 September 2015
Received in revised form 15 February 2016
Accepted 17 February 2016
Available online 18 February 2016

Keywords:
MCU
MICU1
MICU2
Aequorin
HeLa cells
Calcium

ABSTRACT

MICU1 and MICU2 are the main regulators of the mitochondrial Ca^{2+}-uniporter (MCU), but their precise functional role is still under debate. We show here that MICU2 behaves as a pure inhibitor of MCU at low cytosolic $[Ca^{2+}]$ ($[Ca^{2+}]_c$), though its effects decrease as $[Ca^{2+}]_c$ is increased and disappear above 7 μM. Regarding MICU1, studying its effects is more difficult because knockdown of MICU1 leads also to loss of MICU2. However, while knockdown of MICU2 induces only a persistent increase in mitochondrial Ca^{2+} uptake, knockdown of MICU1 also induces a peculiar use-dependent transient activation of MCU that cannot be attributed to the parallel loss of MICU2. Therefore, MICU1 is endowed with a specific inhibitory effect on MCU at low $[Ca^{2+}]_c$, separate and kinetically different from that of MICU2. On the other hand, we and others have shown previously that MICU1 activates MCU at $[Ca^{2+}]_c$ above 2.5 μM. Thus, MICU1 has a double role in MCU regulation, inhibitory at low $[Ca^{2+}]_c$ and activatory at high $[Ca^{2+}]_c$.

1. Introduction

In the last 5 years we have gone from knowing nothing on the molecular substrate of the mitochondrial calcium uniporter to the overwhelming complexity of the present picture of the uniporter, with a main pore subunit, MCU [1,2], which is apparently modulated somehow by other 5 accessory proteins: MCUb [3], EMRE [4], MICU1 [5], MICU2 [6] and MICUR1 [7]. The functional connections between the different subunits have been now partially determined (for recent reviews see [8–13]), but many questions still remain unclear on the role that each of them plays in the regulation of mitochondrial Ca^{2+} uptake.

This paper is mainly concerned with the role of the proteins MICU1 and MICU2 in the regulation of mitochondrial Ca^{2+} uptake. MICU1 was actually the first of the components of the complex to be described [5]. In that work, MICU1 was shown to be required for mitochondrial Ca^{2+} uptake (its knockdown largely reduced it). However, later work indicated that the real role of MICU1 was to act as a gatekeeper of MCU at low cytosolic $[Ca^{2+}]$, so that removal of MICU1 largely increased mitochondrial Ca^{2+} uptake [14]. In addition to that, it was then shown that MICU1 loss attenuated the mitochondrial response to agonist-induced cytosolic $[Ca^{2+}]$ pulses [15]. This suggested that MICU1 could have a different role at low or high $[Ca^{2+}]_c$, either gatekeeper at low $[Ca^{2+}]_c$ or activating at high $[Ca^{2+}]_c$. Using permeabilized cells, we then confirmed this double role, showing that MICU1 knockdown increased mitochondrial Ca^{2+} uptake at $[Ca^{2+}]_c$ below 2.5 μM, but reduced it at $[Ca^{2+}]_c$ above that [16]. Moreover, we found an intriguing property of the Ca^{2+} fluxes activated by MICU1 knockdown. In the absence of MICU1, prolonged activation of MCU at low $[Ca^{2+}]_c$ led to a partial inactivation of the channel response to the same range of low $[Ca^{2+}]_c$, therefore a sort of use-dependent inactivation of MCU [16]. Because of this phenomenon, the kinetics of $[Ca^{2+}]_M$ increase in the presence of a low $[Ca^{2+}]_c$ buffer showed a typical overshoot in the MICU1-silenced cells, which was absent in the controls.

MICU2 is a paralog of MICU1 with 27% sequence identity. It was first described as a protein whose silencing resulted in reduced mitochondrial calcium clearance in response to large (50 μM) extramitochondrial calcium pulses [6]. More recently, it was clearly shown by two groups that the presence of MICU2 in the MCU complex strictly required that MICU1 was also present to form a dimer. Instead, MICU1 could be present and modulate the MCU complex in the absence of MICU2 [17,18]. However, both groups had different views on the role of these proteins in the regulation of MCU. Mootha's group proposed that both MICU1 and MICU2 were operating as negative regulators of the pore [18], so that the absence of MICU2 facilitates Ca^{2+} fluxes, but fully unregulated Ca^{2+} uptake occurs only when both MICU1 and MICU2 are removed. Instead, Rizzuto's group proposed that MICU1 and MICU2 exert an opposite effect on MCU activity, with MICU2 acting as a genuine inhibitor and MICU1 stimulating channel opening [17]. Under this perspective, the previously described gatekeeper function of MICU1 at

Abbreviations: $[Ca^{2+}]_M$, mitochondrial $[Ca^{2+}]$; $[Ca^{2+}]_c$, cytosolic $[Ca^{2+}]$; MCU, mitochondrial calcium uniporter.

* Corresponding author.
E-mail address: jalvarez@ibgm.uva.es (J. Alvarez).

http://dx.doi.org/10.1016/j.bbamem.2016.02.022
0005-2736/

low $[Ca^{2+}]_c$ would be just a consequence of the forced loss of MICU2 (the real inhibitor) when MICU1 is absent.

We have studied here in detail the effect of silencing MICU1, MICU2 or both on the kinetics of mitochondrial Ca^{2+} uptake in HeLa cells. Our results confirm that silencing of any of them activates mitochondrial Ca^{2+} uptake at low cytosolic $[Ca^{2+}]$, but we show also that there are important kinetic differences among the Ca^{2+} fluxes obtained after knockdown of MICU1 (and thus also MICU2) or only MICU2, suggesting that MICU1 may also have defined and non-redundant gatekeeping functions at low $[Ca^{2+}]_c$.

2. Experimental procedures

2.1. Cell culture and gene expression and knockdown

HeLa cells were grown in Dulbecco's modified Eagle's medium supplemented with 5% fetal calf serum, 100 i.u. ml^{-1} penicillin and 100 i.u. ml^{-1} streptomycin. The constructs for cytosolic native aequorin, mitochondrially targeted native aequorin, mitochondrially targeted mutated aequorin (Asp119 → Ala) and double mutated aequorin (Asp119 → Ala and Asn28 → Leu), and ER-targeted double mutated aequorin have been described before [19–21]. Human shRNA constructs made to silence the CBARA1 gene (MICU1) and the EFHA1 gene (MICU2), were obtained from Origene, Rockville, USA. As previously described, ref. TF314182C (TGCAGAATCTCCACCATGTGTAGACAACC) was used for silencing of MICU1. Regarding MICU2, the most effective shRNA were ref. TF304833D (MICU2-shRNA1, GCTCATCGTCCTGTCA GACTAGCGGAGTT) and ref. TF304833C (MICU2-shRNA2, ACACAACT CTTCAGATGCGTTTCTTTGGA). The plasmid containing the MICU2 gene (EFHA1) used for rescue experiments was obtained from Origene, Rockville, USA (ref. RC205455). Transfections were carried out using Metafectene (Biontex, Munich, Germany).

MICU1 silencing was always induced by transient (48–72 h) transfection of the corresponding shRNA, as this method was more effective than the stable clones [16]. Controls were also transfected in parallel with a scrambled shRNA. In the case of MICU2, silencing was obtained either by transient transfection of the specific shRNA or by using stable silenced clones generated using puromycin. To measure $[Ca^{2+}]_M$ in the case of transient transfections, the plasmid containing the corresponding type of targeted aequorin, as mentioned above, was cotransfected either with the specific shRNA construct or with the scrambled shRNA used as a control. Cotransfections were made at a 4:1 mass relationship of the shRNA plasmid with respect to the aequorin plasmid, to assure that all the luminescence came from cells transfected with shRNA. Measurements were carried out 48–72 h after transfection. In the case of the stable silenced clone, cells were transfected with the corresponding aequorin construct, and a stable clone expressing a scrambled shRNA cassette was used as a control.

Transient transfection of the two MICU2-shRNA used produced similar changes in mitochondrial Ca^{2+} uptake. However, the magnitude of the changes was always much larger in the stable clones, and transient transfection of the MICU2-shRNA1 stable clone with the MICU2-shRNA2 still potentiated further the changes. The degree of MICU2 knockdown was measured in the stable clones by western blot, using the polyclonal antibody anti-EFHA1 (Abcam, ab101465) to recognize MICU2 in the cell extracts. Radio Immunoprecipitation Assay (RIPA) buffer was used for cell lysis. Proteins separated in 12% SDS-PAGE (Bio-Rad) were transferred onto polyvinylidene difluoride (PVDF) membranes and assayed with the polyclonal antibody anti-EFHA1 (dilution 1/250). Monoclonal Anti-actin antibody (BD sciences; dilution 1:10,000) was used as the loading control, and was added in a separate lane to avoid overlap with the MICU2 band. Isotype matched, horseradish-peroxidase-conjugated (Amersham; dilution 1:10,000) was used as secondary antibody, followed by detection by chemiluminescence (Bio-Rad).

2.2. $[Ca^{2+}]_M$ measurements with aequorin

HeLa cells were plated onto 13 mm round coverslips prior transfection. For aequorin reconstitution, HeLa cells were incubated for 1–2 h at room temperature in standard medium (145 mM NaCl, 5 mM KCl, 1 mM $MgCl_2$, 1 mM $CaCl_2$, 10 mM glucose, and 10 mM HEPES, pH 7.4) with 1 μM native coelenterazine (for native cytosolic aequorin, native mitochondrial aequorin, mutated mitochondrial aequorin and double mutated mitochondrial aequorin when using $[Ca^{2+}]$ buffers below 7 μM) or coelenterazine i (for double mutated aequorin in ER or in mitochondria when using 7 or 10 μM $[Ca^{2+}]$ buffers). After reconstitution, cells were placed in the perfusion chamber of a purpose-built luminometer. Then, for experiments in intact cells, cells were perfused with standard medium containing 1 mM $[Ca^{2+}]$ followed by the stimuli. For experiments with permeabilized cells, standard medium containing 0.5 mM EGTA instead of Ca^{2+} was perfused for 1 min, followed by 1 min of intracellular medium (130 mM KCl, 10 mM NaCl, 1 mM $MgCl_2$, 1 mM potassium phosphate, 0.5 mM EGTA, 1 mM ATP, 20 μM ADP, 5 mM L-malate, 5 mM glutamate, 5 mM succinate, 20 mM Hepes, pH 7) containing 100 μM digitonin. Then, intracellular medium without digitonin was perfused for 5 min, followed by solutions of known $[Ca^{2+}]$ obtained using either EGTA/Ca^{2+} (for $[Ca^{2+}]$ below 1 μM) or HEDTA/Ca^{2+}/Mg^{2+} (for $[Ca^{2+}]$ above 1 μM) mixtures. Temperature was set at 37 °C. Calibration of the luminescence data into $[Ca^{2+}]$ was made using an algorithm adjusted to the calibration of each aequorin form, as previously described [19,22].

2.3. Measurements of mitochondrial membrane potential

Mitochondrial membrane potential was monitored using the fluorescent indicator tetramethylrhodamine ethyl ester (TMRE). HeLa cells were placed in a cell chamber in the stage of a Zeiss Axiovert 200 microscope under continuous perfusion, permeabilized as described above and then perfused with intracellular medium containing 5 nM TMRE until a steady-state fluorescence was reached (usually about 5 min). Single cell fluorescence was excited at 540 nm using a Cairn monochromator and images of the fluorescence emitted between 570 and 630 nm obtained with a 40× Fluar objective were recorded by a Roper CoolSnap fx camera. Single cell fluorescence records were analyzed off-line using the Imaging Workbench 6.0 program. Experiments were performed at 37 °C using an on-line heater from Harvard Apparatus.

Statistical significance was determined using two-sample Student's t-test. Significance is indicated as: *, $p < 0.05$; **, $p < 0.01$; ***, and $p < 0.005$.

2.4. Materials

Native coelenterazine and coelenterazine i were obtained from Biotium Inc., Hayward, CA, U.S.A. CGP37157 and kaempferol were from Tocris, Bristol, UK. Other reagents were from Sigma, Madrid, Spain or Merck, Darmstadt, Germany.

3. Results

3.1. Effects of MICU2 knockdown on cytosolic and mitochondrial $[Ca^{2+}]$

We have explored in this paper the functional role of the MICU2 protein and its complex interaction with MICU1 in order to regulate Ca^{2+} fluxes through the mitochondrial Ca^{2+} uniporter. As previously described [17], silencing of MICU2 induced a very large increase in the mitochondrial $[Ca^{2+}]$ peak triggered by histamine, an effect which was fully rescued after a 24 h-overexpression of the MICU2 gene (Fig. 1a, statistics in Fig. 1c). This effect was due to a primary increase in mitochondrial Ca^{2+} uptake, because the histamine-induced cytosolic $[Ca^{2+}]$ peak was in fact notably reduced (Fig. 1b, statistics in Fig. 1e).

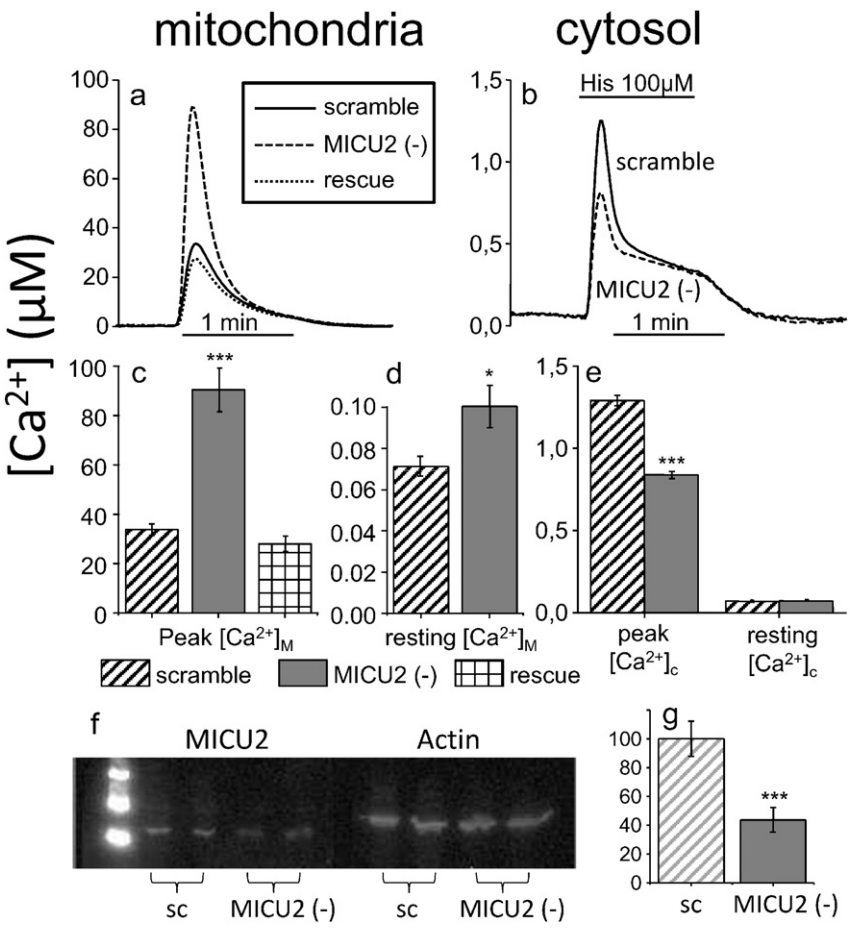

Fig. 1. Effect of MICU2 knockdown on the mitochondrial and cytosolic [Ca^{2+}] peaks induced by histamine. Panel a shows the $[Ca^{2+}]_M$ peaks induced by 100 μM histamine in the MICU2-silenced stable HeLa cell clone MICU2-shRNA1 (MICU2(−)) compared with a scrambled-shRNA cell clone. Overexpression of the MICU2 gene in the MICU2-silenced cell clone fully reverted the effect (panel a, rescue). Panel c shows the statistics of the peaks of panel a (traces are mean ± s.e., n = 11–12). Panel b shows the cytosolic [Ca^{2+}] peaks in the same cell clones, with the corresponding statistics in panel e (traces are mean ± s.e., n = 14–15). Panel d shows the increase in the resting $[Ca^{2+}]_M$ values induced by MICU2-silencing (mean ± s.e., n = 8). Cells were transfected with either mitochondrially targeted mutated aequorin (panel a), cytosolic aequorin (panel b) or mitochondrially targeted native aequorin for the measurement of the resting $[Ca^{2+}]_M$ values (panel d). Panels f–g show the silencing obtained in the MICU2-shRNA1 cell clone compared with the cell clone expressing the scramble shRNA. Statistics shows the mean ± s.e. of 6 determinations. ***, $p < 0.005$.

However, under resting conditions, we could only detect a small but significant increase in $[Ca^{2+}]_M$ in the MICU2-silenced cells, from 71 ± 5 nM to 100 ± 10 nM (mean ± s.e., n = 8, Fig. 1d). Instead, there was no change in the resting $[Ca^{2+}]_c$ levels in the MICU2-silenced cells (Fig. 1e). The degree of MICU2 silencing was measured by western blot. Fig. 1f–g shows that MICU2 was reduced in the MICU2-shRNA1 clone to about 40% of the values in the scrambled clone.

3.2. MICU1 and MICU2 knockdown exert opposite effects on ER [Ca^{2+}] release

Regarding the decrease in the histamine-induced $[Ca^{2+}]_c$ peak in the MICU2-silenced cells, an interesting question was if that was due at least in part to changes in ER-Ca^{2+} release. The increase in mitochondrial Ca^{2+} uptake in the MICU2-silenced cells should lead to a faster buffering of the local high [Ca^{2+}] microdomains around the $InsP_3$ receptors, thus reducing Ca^{2+}-dependent autoinhibition of the channels. In fact, that was the case (see Fig. 2). As we have previously reported [23,24], ER Ca^{2+} release has two phases in control HeLa cells (sc): an initial fast Ca^{2+} release, followed by a slower phase of release. Our hypothesis was that the transition among these phases was due to inhibition by cytosolic Ca^{2+} of the $InsP_3$ receptors [23,24]. Consistently, in the MICU2 silenced cells (MICU2(−)), with a larger mitochondrial Ca^{2+} buffering, the transition disappeared and the fast phase of Ca^{2+} release continued until the maximum release was attained. We had obtained before similar effects by stimulating directly the Ca^{2+} uniporter with kaempferol or other compounds [24]. Fig. 2 also shows the effect of MICU1 silencing on ER-Ca^{2+} release (panels c and d). Interestingly, knockdown of MICU1 produced the opposite effect, that is, a reduction in the rate of ER Ca^{2+} release. Our interpretation here is that the absence of MICU1 reduces mitochondrial Ca^{2+} uptake from the high-Ca^{2+} microdomains generated around $InsP_3R$ during Ca^{2+} release. This increases the feedback inhibition of $InsP_3R$ by the local [Ca^{2+}], slowing Ca^{2+} release.

3.3. MICU2 silencing increases mitochondrial Ca^{2+} uptake only at cytosolic [Ca^{2+}] of 5 μM or below

We have then made a detailed study of the effects of MICU2 silencing on mitochondrial Ca^{2+} uptake in a whole range of cytosolic [Ca^{2+}]. Fig. 3, panels a–h (statistics in panels j–l) shows the changes in mitochondrial Ca^{2+} uptake induced in permeabilized cells by perfusion of [Ca^{2+}] buffers going from 100 nM to 10 μM, and comparing cells expressing a scrambled shRNA (sc) and MICU2-silenced cells (MICU2(−)). It can be observed that mitochondrial Ca^{2+} uptake was largely increased in the MICU2-silenced cells, but only at low cytosolic [Ca^{2+}], from 100 nM to 4.5 μM. Above these levels, at 7 and 10 μM $[Ca^{2+}]_c$, the rate of mitochondrial Ca^{2+} uptake was not significantly

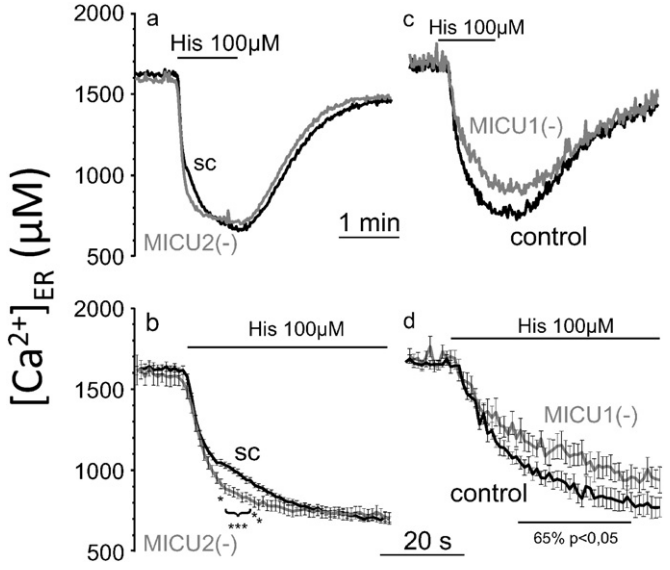

Fig. 2. Effect of MICU2 and MICU1 knockdown on the rate of histamine-induced ER-Ca^{2+} release. Panel a shows the Ca^{2+}-release from the ER induced by histamine in the MICU2-silenced stable HeLa cell clone MICU2-shRNA1 (MICU2(−)) compared with a scrambled-shRNA cell clone (sc), both clones transfected with ER-targeted double-mutated aequorin. Traces are mean ± s.e., n = 13–17. Panel c shows the Ca^{2+}-release from the ER induced by histamine in HeLa cells transiently cotransfected with MICU1-shRNA and ER-targeted double-mutated aequorin (MICU1(−)), compared with cells transfected only with ER-targeted double-mutated aequorin (control). Traces are mean ± s.e., n = 10. Panels b and d show enhanced views of the same traces of the panels above, including the error bars and significances. In the case of panel d, a significant difference among the control and the trace of MICU1-silenced cells was found in 65% of the points in the marked region.

modified by MICU2-silencing. In fact, the effect of MICU2 decreased progressively as $[Ca^{2+}]_c$ was increased. Fig. 3m shows the ratio among the increase in $[Ca^{2+}]_M$ observed in MICU2-silenced cells and that found in the controls. The ratio starts at about 6-fold and decreases steadily as the $[Ca^{2+}]_c$ increases, reaching values close to unity at 7–10 μM. Therefore, these results indicate that MICU2 acts as an inhibitor of the uniporter, but only at low $[Ca^{2+}]_c$ and their effects disappear as the cytosolic $[Ca^{2+}]$ is increased. The effects of MICU2-silencing were not due to changes in mitochondrial membrane potential, because addition of Ca^{2+} to permeabilized cells produced the same changes in TMRE fluorescence both in scramble and MICU2-knockdown cells (Fig. 3i).

It is important to note the kinetics of the $[Ca^{2+}]_M$ increase. The increase in $[Ca^{2+}]_M$ observed in the MICU2-silenced cells reached essentially flat final steady-state values of $[Ca^{2+}]_M$ at all the cytosolic $[Ca^{2+}]$ tested. This contrasts with the large overshoot observed when similar experiments are made with MICU1-silenced cells (see [16] and also Figs. 5 and 6). This important kinetic difference among the activation of mitochondrial Ca^{2+} uptake by knockout of either MICU1 or MICU2 suggests that the activation of mitochondrial Ca^{2+} uptake in MICU1-silenced cells cannot just be attributed to MICU2 removal induced by the absence of MICU1.

3.4. The effects of MICU2-knockdown were unrelated with those of CGP37157 or kaempferol

We have then investigated if the increase in mitochondrial Ca^{2+} uptake induced by MICU2-silencing was somehow related to other two mechanisms we know to increase mitochondrial Ca^{2+} uptake without changing $[Ca^{2+}]_c$. First, inhibiting mitochondrial Ca^{2+} release with the mitochondrial Na^+/Ca^{2+} exchanger inhibitor CGP37157, and second using kaempferol, an activator of the uniporter whose mechanism of action is still unknown [25]. In the case any of these mechanisms was related with the effect of MICU2-silencing, we should obtain a much larger effect of the compound in the controls than in the silenced cells. However, Fig. 4 shows that both CGP37157 (panel a, statistics in panel c) and kaempferol (panel b, statistics in panel d) increased mitochondrial Ca^{2+} uptake similarly in the controls and in the silenced cells, indicating that the effects are additive and thus the activating effect of MICU2 removal is unrelated to the effect of these compounds.

3.5. Differential roles of MICU1 and MICU2 in the modulation of MCU

The interaction between MICU1 and MICU2 and their precise roles in the modulation of Ca^{2+} flux through the MCU protein are still under debate. The main difficulty to investigate this point relies on the fact that MICU2 can only join the MCU complex forming a heterodimer with MICU1, and thus knocking out MICU1 also leads to the loss of MICU2 [17,18]. Instead, MICU1 is able to join the complex alone or forming homodimers. In Fig. 5a (statistics in Fig. 5c) we compare the efficiency of MICU2-silencing under several conditions from the effect it induces in mitochondrial Ca^{2+} uptake. We have used two different MICU2-shRNA obtained from Origene (named 1 and 2 here, see Experimental procedures). Both MICU2-shRNA produced similar but relatively small effects after transient transfections (data not shown), but were much more active after stable expression. Fig. 5a shows the mitochondrial Ca^{2+} uptake induced after transient MICU2-shRNA2 transfection (trace 2), in a MICU2-shRNA1 stable clone (trace 3) or by added MICU2-shRNA2 transfection of the same MICU2-shRNA1 stable clone (trace 4). A stable clone expressing a scrambled shRNA was used as a control (trace 1). The increase in mitochondrial Ca^{2+} uptake induced by MICU2-silencing was much larger in the clone than in the transient transfection, although silencing was still not complete in the MICU2-shRNA1 clone. Western-blot measurements of MICU2 expression in the clone showed a 60% reduction (Fig. 1e–f). In fact, the rate of $[Ca^{2+}]_M$ increase was further enhanced by transient transfection of the clone with the MICU2-shRNA2. The large increase in mitochondrial Ca^{2+} uptake obtained in this last condition (15-fold over the control value in the figure) suggests that a very high degree of silencing has been reached.

Fig. 5b (statistics in panel d) shows a comparison of the effects of MICU1- and MICU2-silencing, and it is quite clear that the kinetics of mitochondrial Ca^{2+} uptake in the MICU2-shRNA1 clone (trace 3) was very different from that obtained after MICU1-shRNA silencing (trace 5). First, the initial rate of Ca^{2+} uptake was much faster after MICU1-silencing (more than two-fold, see panel d). Then, while $[Ca^{2+}]_M$ in the MICU2-shRNA1 clone reached a steady state, in the MICU1-silenced cells it rapidly decreased after an initial overshoot, so that $[Ca^{2+}]_M$ ended up well below that in the MICU2-shRNA1 clone. On the other hand, when the MICU2-shRNA1 clone (trace 3) was transfected with the MICU1-shRNA (trace 6), the rate of mitochondrial Ca^{2+} uptake was largely increased and the initial overshoot appeared, suggesting a summation of two different activating effects.

To investigate further these kinetic differences, we have performed similar experiments but with two consecutive additions of a Ca^{2+} buffer. We have shown before that the $[Ca^{2+}]_M$ overshoot that appears in MICU1-silenced cells is largely suppressed in the second Ca^{2+} addition [16]. Fig. 6a shows that in the case of MICU2 silencing there were little differences among the mitochondrial Ca^{2+} uptake in the first and the second Ca^{2+} addition. No significant differences were found in the maximum increase in $[Ca^{2+}]_M$ (Fig. 6b) and the rate of $[Ca^{2+}]_M$ increase (Fig. 6c) showed only a small reduction that was significant only in the case of the MICU2-shRNA1 clone (trace 3). Instead, as previously shown [16], large differences among the first and the second $[Ca^{2+}]_M$ response were found in MICU1-silenced cells (Fig. 6d, trace 5). Both the maximum value of $[Ca^{2+}]_M$ (Fig. 6e) and the rate of $[Ca^{2+}]_M$ increase (Fig. 6f) were considerably reduced in the second stimulation. Finally, when the MICU2-shRNA1 clone was transfected with the MICU1-shRNA (Fig. 6d, trace 6), the $[Ca^{2+}]_M$ overshoot was similar, but the non-inactivating $[Ca^{2+}]_M$ increase was larger, suggesting again a summation of two separate effects.

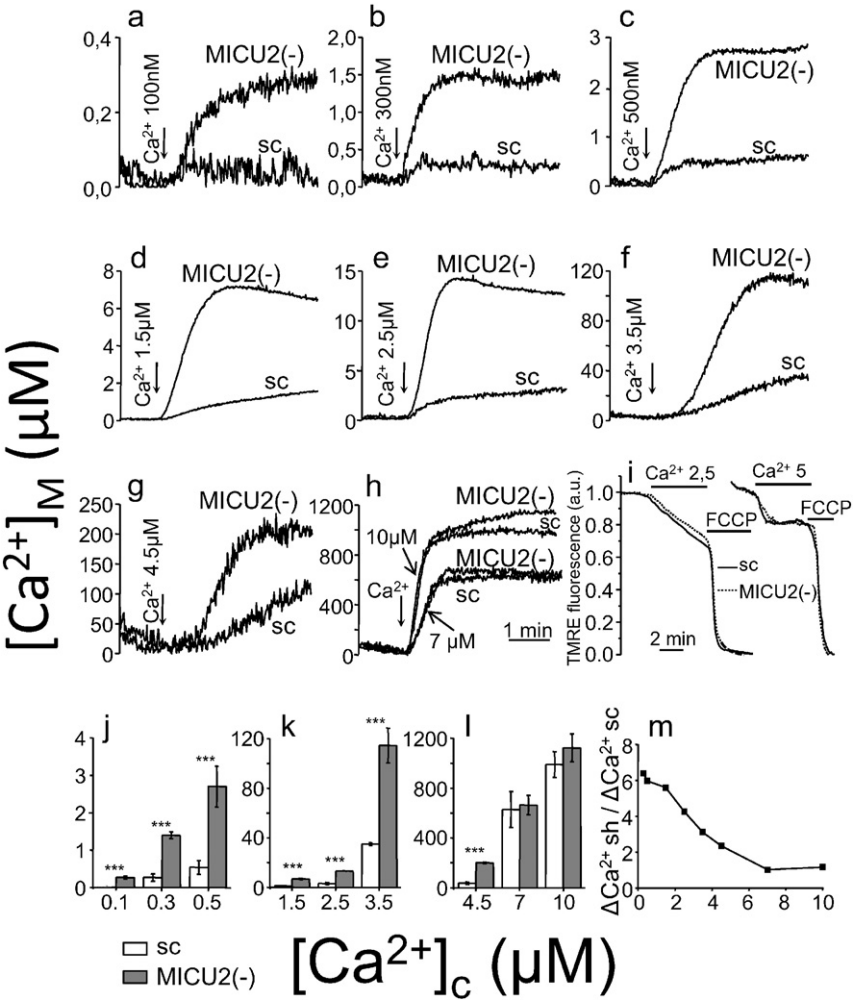

Fig. 3. Effect of MICU2-knockdown on mitochondrial Ca^{2+} uptake in permeabilized cells. The MICU2-silenced stable HeLa cell clone MICU2-shRNA1 (MICU2(−)) and the scrambled-shRNA cell clone (sc) were transfected with mitochondrially-targeted mutated (for panels a–e) or double mutated (for panels f–h) aequorin. Then, they were permeabilized and perfused with Ca^{2+} buffers of known $[Ca^{2+}]$ from 100 nM to 10 μM, as indicated. Traces are the mean of 3–4 different experiments of each type. Panel i shows the effect of Ca^{2+} 2.5 μM, Ca^{2+} 5 μM and FCCP 2 μM on the TMRE fluorescence of permeabilized scramble and MICU2-shRNA1 cells. The traces are the mean of 299 (Ca^{2+} 2.5 μM, scramble), 351 (Ca^{2+} 2.5 μM, MICU2-shRNA1), 420 (Ca^{2+} 5 μM, scramble) and 270 (Ca^{2+} 5 μM, MICU2-shRNA1) single cells analyzed. Panels j–l show the mean ± s.e. of the maximum $[Ca^{2+}]_M$ reached in each case and the significance of the changes induced by MICU2-knockdown at each $[Ca^{2+}]_c$. Panel m shows the ratio of the $[Ca^{2+}]_M$ reached in the MICU2-knockdown clone with respect to the control, and how it decreases progressively when the $[Ca^{2+}]$ in the perfusion buffer increases.

4. Discussion

The mitochondrial Ca^{2+} uniporter has revealed in the last years a surprising complexity in its molecular nature. Apart from the MCU protein, that forms the pore across the inner mitochondrial membrane, several additional proteins have been shown to be associated with it, modulating its activity [8–13]. Reconstitution experiments have shown that the only proteins essential to obtain Ca^{2+} fluxes are MCU and EMRE [26]. However, most mammalian tissues have also MICU1 and MICU2, although their expression is variable and MICU1 has a significantly broader expression pattern than MICU2 [6,27]. This means that many tissues have both regulatory proteins, while some others have only MICU1. Other components of the uniplex are the dominantly negative pore-forming subunit MCUb [3] and the regulatory protein MCUR1 [7], which has been recently shown to interact with the N-terminal domain of MCU [28].

The functional role of MICU1 and MICU2 is presently under debate, as we mentioned in the Introduction. In particular, specific knockdown of MICU2 has clearly suggested that MICU2 behaves as an inhibitor of mitochondrial Ca^{2+} uptake [17,18]. However, the role of MICU1 is more controversial, probably because specific removal of MICU1 is not possible, as it always leads also to loss of MICU2.

In this paper we confirm that MICU2 knockdown increases mitochondrial Ca^{2+} uptake at relatively low $[Ca^{2+}]_c$, below 5 μM. In fact, the activating effect of MICU2 removal is maximum at submicromolar $[Ca^{2+}]_c$ and progressively decreases as $[Ca^{2+}]_c$ is increased, so that no effect is obtained at $[Ca^{2+}]_c$ of 7 μM or above (Fig. 3). Consistently, the $[Ca^{2+}]_M$ peak induced by an agonist is increased and the $[Ca^{2+}]_c$ peak is reduced because a larger fraction of the Ca^{2+} released by the ER is accumulated into the mitochondria (Fig. 1). It is interesting to mention that this occurs in spite of the fact that Ca^{2+} release from the ER is faster in the cells with MICU2 knockdown (Fig. 2). The reason for this probably relies in the larger Ca^{2+} uptake by mitochondria, which reduces the size of the local $[Ca^{2+}]$ microdomains close to the $InsP_3$ receptors, thus avoiding their Ca^{2+}-dependent inactivation. The same happens when mitochondrial Ca^{2+} uptake is directly stimulated with kaempferol or other compounds [24]. It was interesting to find that knockdown of MICU1 produced the opposite effect, that is, a reduction in the rate of ER-Ca^{2+} release. This effect can be explained by the same mechanism, because MICU1-silencing reduces mitochondrial Ca^{2+} uptake from the

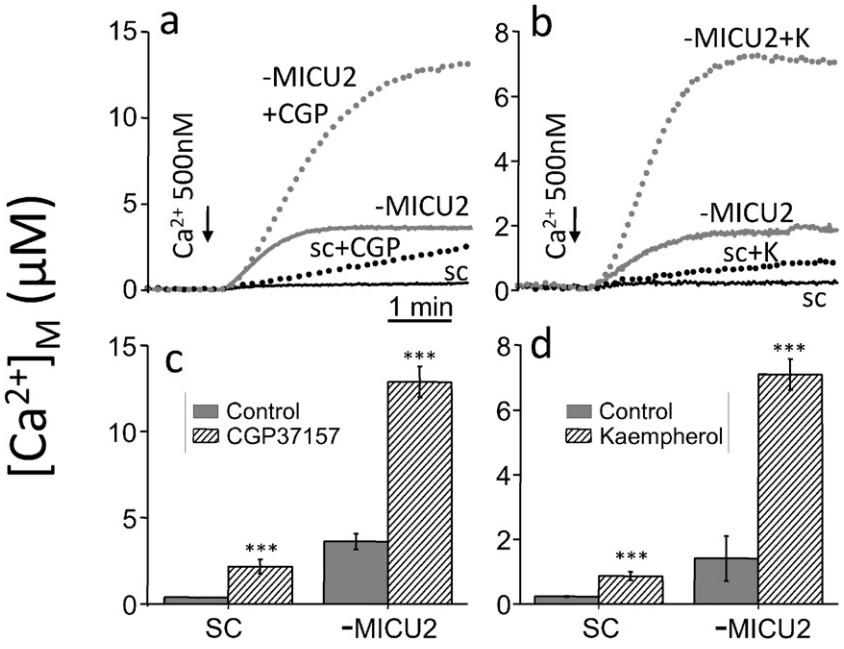

Fig. 4. Effects of CGP37157 and kaempferol on mitochondrial Ca^{2+} uptake in controls and MICU2-silenced cells. The MICU2-silenced stable HeLa cell clone MICU2-shRNA1 (−MICU2) and the scrambled-shRNA cell clone (sc) were transfected with mitochondrially-targeted mutated aequorin, permeabilized and perfused with a 500 nM $[Ca^{2+}]$ buffer, either in the absence or in the presence of 10 μM CGP37157 (CGP, panel a) or 10 μM kaempferol (K, panel b). Traces are the mean of 3–5 similar experiments of each kind. Panels c and d show the mean ± s.e. of the maximum $[Ca^{2+}]_M$ reached in each case and the significance of the changes induced by CGP37157 or kaempferol.

local high-Ca^{2+} microdomains around $InsP_3$ receptors, thus increasing the $[Ca^{2+}]$ of the microdomain and further inhibiting $InsP_3$ receptors. The size of the high-Ca^{2+} microdomains generated close to mitochondria, after histamine stimulation of HeLa cells, has been found to be 5- to 10-fold higher than in the bulk cytosol [29]. Thus, they are well in the range of $[Ca^{2+}]$ values where MICU1 behaves as an activator of MCU (above 2.5 μM, [16]).

The increase in mitochondrial Ca^{2+} uptake induced by MICU2-knockdown was not due to changes in the rate of Ca^{2+} release from mitochondria. Inhibition of the mitochondrial Na^+/Ca^{2+} exchanger with CGP37157 further enhanced the rate of $[Ca^{2+}]_M$ increase, but the difference among controls and MICU2-knockdown cells persisted. Similarly, the mitochondrial Ca^{2+} uniporter activator kaempferol increased the rate of mitochondrial Ca^{2+} entry, but again the difference among

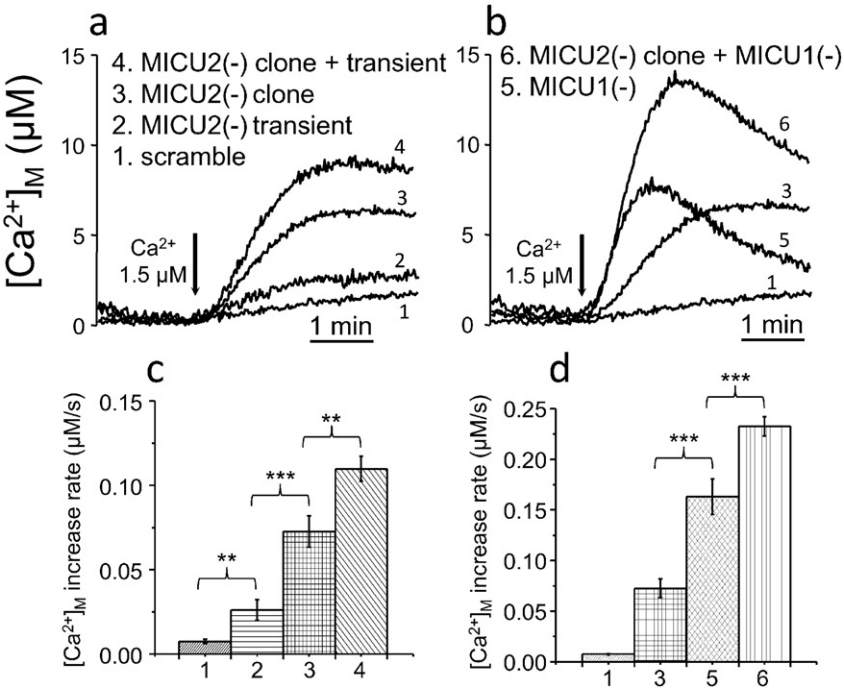

Fig. 5. Effects of MICU1 and MICU2 knockdown on mitochondrial Ca^{2+} uptake. Cells under several conditions were transfected with mitochondrially targeted mutated aequorin, permeabilized and perfused with a 1.5 μM $[Ca^{2+}]$ buffer, as indicated. The conditions were: 1, cell clone expressing scrambled shRNA. 2, transient 72 h transfection with MICU2-shRNA2. 3, stable cell clone expressing MICU2-shRNA1. 4, transient 72 h transfection with MICU2-shRNA2 of the stable cell clone expressing MICU2-shRNA1. 5, transient 72 h transfection with MICU1-shRNA. 6. transient 72 h transfection with MICU1-shRNA of the stable cell clone expressing MICU2-shRNA1. Traces are the mean of 3 different experiments of each kind. Panels c and d show the mean ± s.e. of the rates of $[Ca^{2+}]_M$ increase in each case, and the significance of the changes.

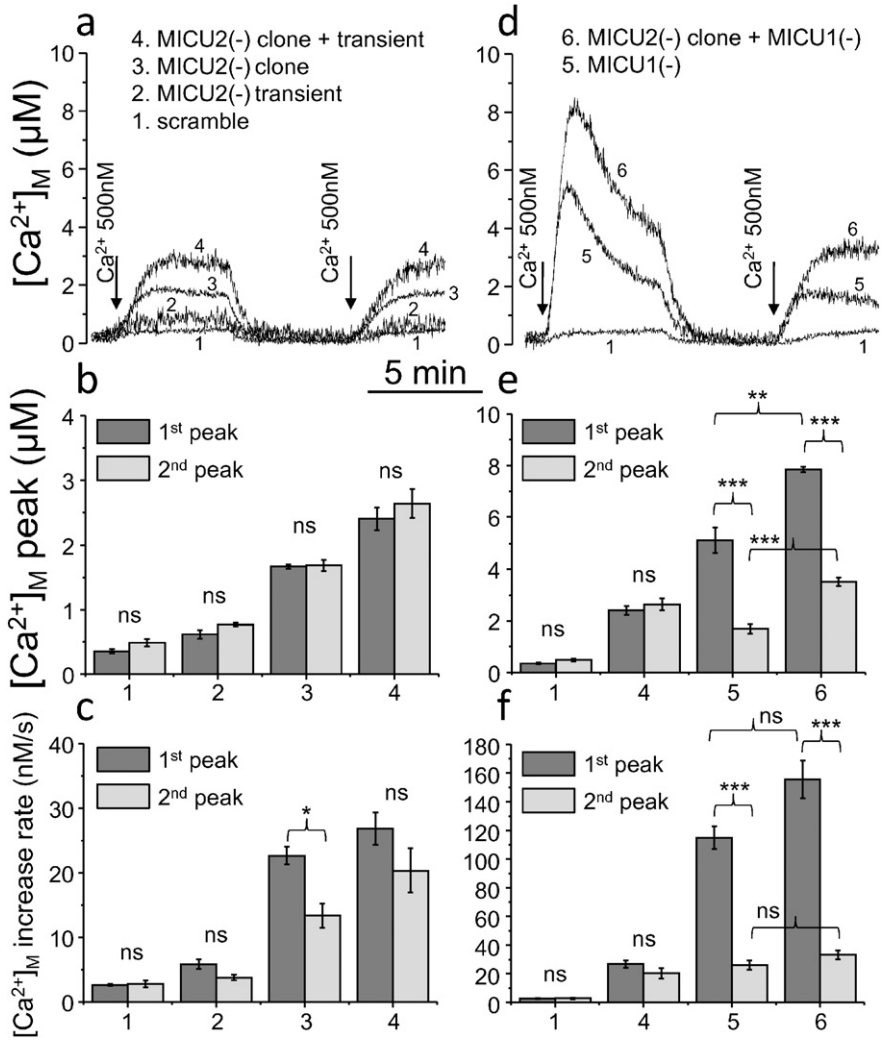

Fig. 6. Effects of MICU1 and MICU2 knockdown on mitochondrial Ca^{2+} uptake during two consecutive stimulations with a [Ca^{2+}] buffer. Permeabilized cells were subjected to two consecutive stimulations with a 500 nM [Ca^{2+}] buffer with a 5 min interval (panels a and d). The different cell conditions were as in Fig. 5. Traces are the mean of 3 different experiments of each kind. Panels b and e show the mean ± s.e. of the maximum $[Ca^{2+}]_M$ increase in each case, and the significance of the changes, as indicated. Panels c and f show the mean ± s.e. of the rates of $[Ca^{2+}]_M$ increase in each case, and the significance of the changes.

the rates in controls and MICU2-knockdown cells persisted. Therefore, the mechanism of activation of the uniporter by kaempferol appears to be unrelated to MICU2 function.

The kinetics of the mitochondrial Ca^{2+} uptake stimulated by MICU2 removal was that of a simple and persistent increase in Ca^{2+} flux through the uniporter, leading to a higher stable steady-state $[Ca^{2+}]_M$ set by the balance among the increased Ca^{2+} uptake and the Ca^{2+} release through the mitochondrial Na^+/Ca^{2+} exchanger, whose rate increases with the $[Ca^{2+}]_M$ level [30]. In fact, inhibition of the mitochondrial Na^+/Ca^{2+} exchanger with CGP37157 largely increased the mitochondrial $[Ca^{2+}]_M$ levels reached (Fig. 4). This kinetics contrasts with that observed after MICU1 knockdown ([16], see also Figs. 5 and 6), where addition of Ca^{2+} induces a fast initial $[Ca^{2+}]_M$ overshoot followed by a more persistent $[Ca^{2+}]_M$ plateau at lower levels. Therefore, activation of the Ca^{2+} pathway in this case has two components, one transient and one permanent.

The protocol of double Ca^{2+} addition of Fig. 6 clearly shows these different patterns, and how the transient response due to MICU1 removal disappears in the second stimulation. Thus, MICU2 knockdown alone triggers a persistent opening of the Ca^{2+} pathway (trace 4). MICU1 knockdown triggers both a transient and a persistent response (trace 5). And finally, transient MICU1 knockdown of the MICU2-knockdown clone (trace 6) generates the same Ca^{2+} overshoot as that in trace 5, but with an increased persistent response. The hypothesis we propose to explain these experiments is that MICU2 removal must be responsible for the persistent increase in mitochondrial Ca^{2+} uptake obtained at low cytosolic [Ca^{2+}]. MICU1 removal, on the other hand, would be responsible for the transient and use-dependent opening of the Ca^{2+} pathway in the same conditions. However, as MICU1 removal also leads to MICU2 depletion from the MCU complex, the final effect of MICU1 knockdown is both a transient and a persistent increase in mitochondrial Ca^{2+} uptake. In the case of traces 5 and 6 of Fig. 6d (MICU1 knockdown on either wild type cells or a MICU2-knockdown clone), the transient response is the same because the silencing effect of the MICU1-shRNA is the same in both cases. However, as the silencing is not complete, a percentage of the MCU proteins remains coupled to MICU1 and MICU2 after single MICU1 knockdown. This option corresponds to trace 5 of Fig. 6d, where we have either MCU proteins with both MICU1 and MICU2, or with none of them. Instead, if MICU1 knockdown is performed in the MICU2 knockdown cell clone, depletion of MICU1 (+MICU2) will be similar, but many of the remaining MCU–MICU1 complexes will be also depleted of MICU2, generating the additive response we see in trace 6 of Fig. 6d. Here we have a few MCU proteins with both MICU1 and MICU2, others with only MICU1, probably as a homodimer [17], and as many as in trace 5 with none of them.

In conclusion, we show here that knockdown of MICU1 produces a transient, use-dependent, activation of MCU that cannot be attributed to the parallel loss of MICU2. Therefore, MICU1 cooperates with MICU2 to keep closed and set the threshold of MCU activation at low $[Ca^{2+}]_c$. Both regulators thus act as inhibitors of the MCU at low $[Ca^{2+}]_c$. However, their effects change at high $[Ca^{2+}]_c$. As we have reported before [16], MICU1 behaves as an activator of MCU at $[Ca^{2+}]_c$ above 2.5 μM. Regarding MICU2, we show here that its removal produces no effects at $[Ca^{2+}]_c$ of 7 μM and above. Therefore, MICU2 is a genuine inhibitor of MCU, though only at low $[Ca^{2+}]_c$, and MICU1 has a double role, inhibitory at low $[Ca^{2+}]_c$ and activatory at high $[Ca^{2+}]_c$.

Acknowledgments

This work was supported by grants from the Spanish Ministerio de Ciencia e Innovación [BFU2011-25763] and Ministerio de Economía y Competitividad [BFU2014-55731-R]. Jessica Matesanz-Isabel holds an FPI (Formación de Personal Investigador, BES-2012-053044) fellowship from the Spanish Government and Jessica Arias-del-Val has a fellowship from Junta de Castilla y Leon (EDU/1083/2013).

References

[1] D. De Stefani, A. Raffaello, E. Teardo, I. Szabò, R. Rizzuto, A forty-kiloDalton protein of the inner membrane is the mitochondrial calcium uniporter, Nature 476 (2011) 336–340.
[2] J.M. Baughman, F. Perocchi, H.S. Girgis, M. Plovanich, C.A. Belcher-Timme, Y. Sancak, X.R. Bao, L. Strittmatter, O. Goldberger, R.L. Bogorad, V. Koteliansky, V.K. Mootha, Integrative genomics identifies MCU as an essential component of the mitochondrial calcium uniporter, Nature 476 (2011) 341–345.
[3] A. Raffaello, D. De Stefani, D. Sabbadin, E. Teardo, G. Merli, A. Picard, V. Checchetto, S. Moro, I. Szabò, R. Rizzuto, The mitochondrial calcium uniporter is a multimer that can include a dominant-negative pore-forming subunit, EMBO J. 32 (2013) 2362–2376.
[4] Y. Sancak, A.L. Markhard, T. Kitami, E. Kovács-Bogdán, K.J. Kamer, N.D. Udeshi, S.A. Carr, D. Chaudhuri, D.E. Clapham, A.A. Li, S.E. Calvo, O. Goldberger, V.K. Mootha, EMRE is an essential component of the mitochondrial calcium uniporter complex, Science 342 (2013) 1379–1382.
[5] F. Perocchi, V.M. Gohil, H.S. Girgis, X.R. Bao, J.E. McCombs, A.E. Palmer, V.K. Mootha, MICU1 encodes a mitochondrial EF hand protein required for Ca^{2+} uptake, Nature 467 (2010) 291–296.
[6] M. Plovanich, R.L. Bogorad, Y. Sancak, K.J. Kamer, L. Strittmatter, A.A. Li, H.S. Girgis, S. Kuchimanchi, J. De Groot, L. Speciner, N. Taneja, J. Oshea, V. Koteliansky, V.K. Mootha, MICU2, a paralog of MICU1, resides within the mitochondrial uniporter complex to regulate calcium handling, PLoS One 8 (2013), e55785.
[7] K. Mallilankaraman, C. Cárdenas, P.J. Doonan, H.C. Chandramoorthy, K.M. Irrinki, T. Golenár, G. Csordás, P. Madireddi, J. Yang, M. Müller, R. Miller, J.E. Kolesar, J. Molgó, B. Kaufman, G. Hajnóczky, J.K. Foskett, M. Madesh, MCUR1 is an essential component of mitochondrial Ca^{2+} uptake that regulates cellular metabolism, Nat. Cell Biol. 14 (2012) 1336–1343.
[8] D. Chaudhuri, Y. Sancak, V.K. Mootha, D.E. Clapham, MCU encodes the pore conducting mitochondrial calcium currents, Elife 2 (2013), e00704.
[9] K.J. Kamer, Y. Sancak, V.K. Mootha, The uniporter: from newly identified parts to function, Biochem. Biophys. Res. Commun. 449 (2014) 370–372.
[10] D. De Stefani, R. Rizzuto, Molecular control of mitochondrial calcium uptake, Biochem. Biophys. Res. Commun. 449 (2014) 373–376.
[11] J.K. Foskett, M. Madesh, Regulation of the mitochondrial Ca^{2+} uniporter by MICU1 and MICU2, Biochem. Biophys. Res. Commun. 449 (2014) 377–383.
[12] D. Pendin, E. Greotti, T. Pozzan, The elusive importance of being a mitochondrial Ca^{2+} uniporter, Cell Calcium 55 (2014) 139–145.
[13] D. De Stefani, M. Patron, R. Rizzuto, Structure and function of the mitochondrial calcium uniporter complex, Biochim. Biophys. Acta 1853 (2015) 2006–2011.
[14] K. Mallilankaraman, P. Doonan, C. Cárdenas, H.C. Chandramoorthy, M. Müller, R. Miller, N.E. Hoffman, R.K. Gandhirajan, J. Molgó, M.J. Birnbaum, B.S. Rothberg, D.O. Mak, J.K. Foskett, M. Madesh, MICU1 is an essential gatekeeper for MCU-mediated mitochondrial Ca^{2+} uptake that regulates cell survival, Cell 151 (2012) 630–644.
[15] G. Csordás, T. Golenár, E.L. Seifert, K.J. Kamer, Y. Sancak, F. Perocchi, C. Moffat, D. Weaver, S. de la Fuente, R. Bogorad, V. Koteliansky, J. Adijanto, V.K. Mootha, G. Hajnóczky, MICU1 controls both the threshold and cooperative activation of the mitochondrial Ca^{2+} uniporter, Cell Metab. 17 (2013) 976–987.
[16] S. de la Fuente, J. Matesanz-Isabel, R.I. Fonteriz, M. Montero, J. Alvarez, Dynamics of mitochondrial Ca^{2+} uptake in MICU1-knockdown cells, Biochem. J. 458 (2014) 33–40.
[17] M. Patron, V. Checchetto, A. Raffaello, E. Teardo, D. Vecellio Reane, M. Mantoan, V. Granatiero, I. Szabò, D. De Stefani, R. Rizzuto, MICU1 and MICU2 finely tune the mitochondrial Ca^{2+} uniporter by exerting opposite effects on MCU activity, Mol. Cell 53 (2014) 726–737.
[18] K.J. Kamer, V.K. Mootha, MICU1 and MICU2 play nonredundant roles in the regulation of the mitochondrial calcium uniporter, EMBO Rep. 15 (2014) 299–307.
[19] M. Brini, R. Marsault, C. Bastianutto, J. Alvarez, T. Pozzan, R. Rizzuto, Transfected aequorin in the measurement of cytosolic Ca^{2+} concentration ($[Ca^{2+}]_c$). A critical evaluation, J. Biol. Chem. 270 (1995) 9896–9903.
[20] S. de la Fuente, R.I. Fonteriz, P.J. de la Cruz, M. Montero, J. Alvarez, Mitochondrial free $[Ca^{2+}]$ dynamics measured with a novel low-Ca^{2+} affinity aequorin probe, Biochem. J. 445 (2012) 371–376.
[21] S. de la Fuente, R.I. Fonteriz, M. Montero, J. Alvarez, Ca^{2+} homeostasis in the endoplasmic reticulum measured with a new low-Ca^{2+}-affinity targeted aequorin, Cell Calcium 54 (2013) 37–45.
[22] M. Montero, C.D. Lobatón, A. Moreno, J. Alvarez, A novel regulatory mechanism of the mitochondrial Ca^{2+} uniporter revealed by the p38 mitogen-activated protein kinase inhibitor SB202190, FASEB J. 16 (2002) 1955–1957.
[23] M. Montero, M.J. Barrero, J. Alvarez, $[Ca^{2+}]$ microdomains control agonist-induced Ca^{2+} release in intact HeLa cells, FASEB J. 11 (1997) 881–885.
[24] L. Vay, E. Hernández-SanMiguel, J. Santo-Domingo, C.D. Lobatón, A. Moreno, M. Montero, J. Alvarez, Modulation of Ca^{2+} release and Ca^{2+} oscillations in HeLa cells and fibroblasts by mitochondrial Ca^{2+} uniporter stimulation, J. Physiol. 580 (2007) 39–49.
[25] M. Montero, C.D. Lobatón, E. Hernández-SanMiguel, J. Santo-Domingo, L. Vay, A. Moreno, J. Alvarez, Direct activation of the mitochondrial calcium uniporter by natural plant flavonoids, Biochem. J. 384 (2004) 19–24.
[26] E. Kovács-Bogdán, Y. Sancak, K.J. Kamer, M. Plovanich, A. Jambhekar, R.J. Huber, M.A. Myre, M.D. Blower, V.K. Mootha, Reconstitution of the mitochondrial calcium uniporter in yeast, Proc. Natl. Acad. Sci. U. S. A. 111 (2014) 8985–8990.
[27] D.J. Pagliarini, S.E. Calvo, B. Chang, S.A. Sheth, S.B. Vafai, S.E. Ong, G.A. Walford, C. Sugiana, A. Boneh, W.K. Chen, D.E. Hill, M. Vidal, J.G. Evans, D.R. Thorburn, S.A. Carr, V.K. Mootha, A mitochondrial protein compendium elucidates complex I disease biology, Cell 134 (2008) 112–123.
[28] Y. Lee, C.K. Min, T.G. Kim, H.K. Song, Y. Lim, D. Kim, K. Shin, M. Kang, J.Y. Kang, H.S. Youn, J.G. Lee, J.Y. An, K.R. Park, J.J. Lim, J.H. Kim, J.H. Kim, Z.Y. Park, Y.S. Kim, J. Wang, do H. Kim, S.H. Eom, Structure and function of the N-terminal domain of the human mitochondrial calcium uniporter, EMBO Rep. 16 (2015) 1318–1333.
[29] M. Giacomello, I. Drago, M. Bortolozzi, M. Scorzeto, A. Gianelle, P. Pizzo, T. Pozzan, Ca^{2+} hot spots on the mitochondrial surface are generated by Ca^{2+} mobilization from stores, but not by activation of store-operated Ca^{2+} channels, Mol. Cell 38 (2010) 280–290.
[30] S. de la Fuente, P. Montenegro, R.I. Fonteriz, A. Moreno, C.D. Lobatón, M. Montero, J. Alvarez, The dynamics of mitochondrial Ca^{2+} fluxes, Biochim. Biophys. Acta 1797 (2010) 1727–1735.